COMMUNICATIONS IN COMPUTATIONAL PHYSICS
Vol. **4**, No. 2, pp. 275-293

Commun. Comput. Phys.
August 2008

A Generalized Peierls-Nabarro Model for Curved Dislocations Using Discrete Fourier Transform

He Wei[1,*], Yang Xiang[2] and Pingbing Ming[3]

[1] *School of Mathematical Sciences, Peking University, Beijing 100871, China.*
[2] *Department of Mathematics, The Hong Kong University of Science and Technology, Clear Water Bay, Kowloon, Hong Kong.*
[3] *Institute of Computational Mathematics and Scientific/Engineering Computing, Academy of Mathematics and System Sciences, Chinese Academy of Sciences, No.55 Zhong-Guan-Cun East Road, Beijing 100080, China.*

Received 23 October 2007; Accepted (in revised version) 9 December 2007

Communicated by Weinan E

Available online 18 March 2008

Abstract. In this paper, we present a generalized Peierls-Nabarro model for curved dislocations using the discrete Fourier transform. In our model, the total energy is expressed in terms of the disregistry at the discrete lattice sites on the slip plane, and the elastic energy is obtained efficiently within the continuum framework using the discrete Fourier transform. Our model directly incorporates into the total energy both the Peierls energy for the motion of straight dislocations and the second Peierls energy for kink migration. The discreteness in both the elastic energy and the misfit energy, the full long-range elastic interaction for curved dislocations, and the changes of core and kink profiles with respect to the location of the dislocation or the kink are all included in our model. The model is presented for crystals with simple cubic lattice. Simulation results on the dislocation structure, Peierls energies and Peierls stresses of both straight and kinked dislocations are reported. These results qualitatively agree with those from experiments and atomistic simulations.

AMS subject classifications: 35Q72, 65D05, 74C99, 74G65, 74S25

Key words: Dislocation, Peierls-Nabarro model, Peierls stress, Peierls energy, dislocation kink.

1 Introduction

Dislocations are one-dimensional topological defects in crystalline solids, whose motion is directly responsible for the plastic deformation of these materials [1]. When a straight

*Corresponding author. *Email addresses:* weihe_pku@yahoo.com.cn (H. Wei), maxiang@ust.hk (Y. Xiang), mpb@lsec.cc.ac.cn (P. Ming)

dislocation moves in its slip plane over the crystal lattice, its energy changes periodically, and an energy barrier has to be overcome when it moves from one energy valley to another. This energy barrier is referred to as the Peierls energy, and the minimum stress to drive the dislocation over this energy barrier is the Peierls stress [1–4]. In reality, due to thermal fluctuations and other effects, a dislocation line may lie in different Peierls valleys connected by kinks, and the motion of the dislocation is also controlled by the kink nucleation and migration. The energy barrier and the minimum stress to move an individual kink are the second Peierls energy and the second Peierls stress, respectively [1, 5–12]. These Peierls energies and Peierls stresses play important roles in characterizing the mobility of dislocation lines [1–16, 18–30].

The Peierls energy and Peierls stress can be estimated using the Peierls-Nabarro model [1–4], which is a hybrid model incorporating atomic features into continuum framework. In the Peierls-Nabarro model, the solid is divided by the slip plane of the dislocation into two half-space linear elastic continua, which have a disregistry (or misfit) relative to each other and are connected by a nonlinear potential force. The total energy consists of the elastic energy in the two half-space continua and the misfit energy due to the nonlinear atomic interaction across the slip plane. The minimum energy state gives the dislocation core profile on the slip plane. The change of the energy as the dislocation moves over the crystal lattice is obtained by shifting rigidly the continuous dislocation profile and summing the misfit energy over the discrete lattice sites near the slip plane. The Peierls energy is the difference between the maximum and minimum of this discrete summation of misfit energy, and the Peierls stress is associated with the maximum derivative of this discrete summation of misfit energy.

The estimates of the Peierls energy and Peierls stress within the Peierls-Nabarro model give qualitative descriptions for the energy barrier and minimum stress required when the dislocations move over the crystal lattice, and agree reasonably with the experimental results [1–4, 14–16]. The Peierls-Nabarro model has been improved greatly with the generalized stacking fault energy [17] obtained using *ab initio* calculations [18–23]. However, in most of these models, the estimates of the Peierls energy and Peierls stress are still obtained in the same way as those in the classical Peierls-Nabarro model, which has been criticized for the following limitations [20, 25]. The first limitation is the inconsistency in the incorporation of the lattice discreteness: on one hand, the continuous dislocation core profile is obtained from energy minimization, on the other hand, discrete sum is used to calculate the Peierls energy; i.e., the Peierls energy is not directly included in the energy minimization. Another limitation is that only the discreteness of the misfit energy is considered, while the discreteness of the elastic energy is neglected. Finally, this method is based on the assumption that the dislocation core profile does not change as it moves. It has been shown that these limitations may result in large errors especially in dealing with dislocations with narrow cores (e.g. in silicon) [20, 25].

Several efforts have been made to address these problems. Bulatov and Kaxiras proposed a semidiscrete variational Peierls framework [20], in which the total energy is minimized with respect to the disregistry at discrete lattice sites and the elastic energy is still

obtained in the continuum framework by linking the values of disregistry at discrete lattice sites using piecewise linear functions. This method has been applied to dislocations in Si [20] and Al [23]. Movchan *et al*. [24] proposed a discrete model in which the singular integral in the stress formula is regularized and then evaluated at the discrete lattice sites to include the effect of the crystal lattice. In these models [20, 23, 24], the Peierls stress is calculated as the critical stress at which the procedure of energy minimization fails to converge. Schoeck [25–27] included in the total energy the approximation of the energy change due to the discrete lattice using Poisson's summation formula, and the dislocation profile is obtained using a set of trial functions of the Peierls type. All these models are for straight dislocations.

In the classical models for dislocation kinks [1, 5, 6, 8, 11, 13], a dislocation is approximated by almost straight line segments lying in the Peierls valleys and connected by kinks (the string approximation). Besides the limitations of the classical Peierls-Nabarro model for straight dislocations, further simplifications are needed in these string approximation models for dislocations with kinks. First, the core structure of the dislocation is lost in these models. Second, the long-range elastic effect is only approximated by the local line tension model, and the line tension cannot be determined accurately for a general curved dislocation. Finally, the Peierls energy in the direction normal to the almost straight dislocation is included as a given function obtained from the Peierls-Nabarro model for straight dislocations, which may not be accurate near the kink; while the second Peierls energy for a kink (the energy barrier for kink migration) and the second Peierls stress (the minimum stress to move a kink along the dislocation) are missing in these models. However, it has been shown that the second Peierls energy for kinks is very high and comparable with the Peierls energy for straight dislocations in covalent bond crystals such as Si [19, 28].

Only a few attempts have been made within the frameworks of the Peierls-Nabarro model and the string approximation to calculate the second Peierls stress and the second Peierls energy for dislocation kinks. In the models of Joos *et al*. [9, 10], similar to the Peierls energy for a straight dislocation in the Peierls-Nabarro model, the second Peierls energy for a kink within the string approximation is obtained from the summation of the total energy at discrete lattice sites along the dislocation, and the second Peierls stress is associated with the maximum derivative of the discrete summation of the total energy. Schottky [6] used the long-range elastic interaction in the string approximation in the kink profile, and obtained the second Peierls energy using discrete summation. Sanders [7] calculated kink profile, the second Peierls energy and the second Peierls stress using a two dimensional Frenkel-Kontorowa model, which is a simplified atomistic model considering only the interaction of the atoms on the slip plane, while the whole upper and lower half spaces of atoms are omitted. Movchan *et al*. [29] proposed a two-dimensional lattice model in which the singular integral in the stress formula is regularized and then evaluated at the discrete lattice sites, and used the model to simulate the motion of a dislocation kink; however, they did not give any quantitative estimates for the second Peierls stress or the second Peierls energy. Some generalizations have also

been made by Xu and Argon [31] and Xiang *et al*. [32] on the models for curved dislocations within the Peierls-Nabarro framework. However, the Peierls energies and Peierls stresses are not directly included in these models.

In this paper, using the discrete Fourier transform, we present a generalized Peierls-Nabarro model for curved dislocations incorporating the Peierls energies and Peierls stresses. In our model, the total energy is expressed in terms of the disregistry at the discrete lattice sites on the slip plane, and the elastic energy is obtained efficiently within the continuum framework using the discrete Fourier transform. The latter means that when calculating the elastic fields, the values of the disregistry at discrete lattice sites are connected smoothly using the trigonometric functions. Our model directly incorporates into the total energy the Peierls energy for the motion of straight dislocations and the second Peierls energy for kink migration. The discreteness in both the elastic energy and the misfit energy, the full long-range elastic interaction for curved dislocations, and the changes of core and kink profiles with respect to the location of the dislocation or the kink are all included in our model. In this paper, we present our model for crystals with simple cubic lattice. The core structure and profile of both straight and kinked dislocations, the Peierls energy and Peierls stress for straight dislocations, and the second Peierls energy and Peierls stress will be obtained using our model. We will show that these results qualitatively agree with those from experiments and atomistic simulations.

2 The classical Peierls-Nabarro model for straight dislocations

In this section, we briefly review the classical Peierls-Nabarro model for a straight dislocation and how the Peierls energy and the Peierls stress are calculated within this model. More on this model can be found in [1–4].

As an example, consider an edge dislocation in a crystal with simple cubic lattice. In a Cartesian set of coordinates xyz, assume that the dislocation is located along the y axis and the Burgers vector is in the direction of the x axis. Thus the xy plane is the slip plane of the dislocation. The length of the Burgers vector is b. The disregistry of the upper half crystal ($z>0$) relative to the lower half ($z<0$) in the direction of the Burgers vector is $\phi(x)$, where $\phi(-\infty)=0$ and $\phi(+\infty)=b$. The distribution of the Burgers vector of the edge dislocation is $\rho(x)=\phi'(x)$.

In the Peierls-Nabarro model, the total energy is written as

$$E=E_{\text{elastic}}+E_{\text{misfit}}, \tag{2.1}$$

where

$$E_{\text{elastic}}=\int_{\mathbf{R}^3}\sum_{i,j=1}^{3}\frac{1}{2}\sigma_{ij}\epsilon_{ij}dxdydz \tag{2.2}$$

is the elastic energy in the upper and lower half spaces, $\{\sigma_{ij}\}$ and $\{\epsilon_{ij}\}$ are the stress and strain tensors, respectively, and E_{misfit} is the misfit energy due to the nonlinear atomic

interaction across the slip plane

$$E_{\text{misfit}} = \int_{-\infty}^{+\infty} \gamma(\phi(x))\mathrm{d}x, \tag{2.3}$$

where $\gamma(\phi)$ is the interplanar potential. In the classical Peierls-Nabarro model, isotropic elasticity is used for E_{elastic}, and $\gamma(\phi)$ in E_{misfit} is approximated by the Frenkel sinusoidal potential

$$\gamma(\phi) = \frac{\mu b^2}{4\pi^2 d}\left(1-\cos\frac{2\pi\phi}{b}\right), \tag{2.4}$$

where d is the lattice spacing perpendicular to the slip plane, and μ is the shear modulus. The equilibrium configuration of the dislocation is obtained by minimizing the total energy with respect to $\phi(x)$, which results in the integro-differential equation

$$\frac{\mu}{2\pi(1-\nu)}\int_{-\infty}^{+\infty}\frac{\phi'(x_1)}{x-x_1}\mathrm{d}x_1 = \frac{\mu b}{2\pi d}\sin\frac{2\pi\phi(x)}{b}, \tag{2.5}$$

where ν is Poisson ratio. This equation has an analytical solution

$$\phi(x) = \frac{b}{\pi}\tan^{-1}\frac{x}{\zeta}+\frac{b}{2}, \tag{2.6}$$

where $\zeta = \frac{1}{2}d/(1-\nu)$ is the half-width of the dislocation.

In order to obtain estimates of the energy barrier and the critical stress to move a dislocation using this model, Peierls [2] and Nabarro [3] assumed that the elastic energy in the two half-spaces does not vary when the dislocation moves over the discrete crystal lattice, i.e., the total energy variation as the dislocation moves over the discrete lattice only comes from the change in the misfit energy. They also assumed that the dislocation core profile given by Eq. (2.6) does not change as the dislocation moves. Under these assumptions, the integral in the misfit energy in Eq. (2.3) was replaced by the summation at discrete lattice sites

$$E_{\text{misfit}}(\alpha) = \sum_{n=-\infty}^{+\infty}\frac{b}{2}[\gamma(\phi(nb+\alpha b))+\gamma(\phi(nb+b/2+\alpha b))], \tag{2.7}$$

where αb is the location of the center of the dislocation relative to a reference atomic site, and $\phi(x)$ is given by the solution Eq. (2.6). This summation is the average of the misfit energy at the lattice sites on the rows right above and below the slip plane, which have a shift $b/2$ due to the initial configuration for the energy minimization used in the model. The summation can be approximated to the leading order by

$$E_{\text{misfit}}(\alpha) = \frac{\mu b^2}{4\pi(1-\nu)}\left[1+2\exp(-\frac{4\pi\zeta}{b})\cos 4\pi\alpha\right]. \tag{2.8}$$

The Peierls energy is then defined as the amplitude of the energy variations

$$E_{1p}^{(1)} = \frac{\mu b^2}{\pi(1-\nu)} \exp(-\frac{4\pi\zeta}{b}), \tag{2.9}$$

and the Peierls stress is associated with the maximum derivative of the Peierls energy with respect to the dislocation translation $\max_{\alpha} \frac{1}{b^2} \frac{\partial E_{\text{misfit}}(\alpha)}{\partial \alpha}$, which is

$$\sigma_{1p}^{(1)} = \frac{2\mu}{1-\nu} \exp(-\frac{4\pi\zeta}{b}). \tag{2.10}$$

It has been argued that the period $b/2$ in the misfit energy given by Eq. (2.8) is not physical [4, 16], and that in order to obtain the correct period b, the summing should be performed at the lattice positions after the energy minimization [4] or on a single row of the atoms near the slip plane [16, 19–27]. Both modifications give the misfit energy [4, 16]

$$E_{\text{misfit}}(\alpha) = \frac{\mu b^2}{4\pi(1-\nu)} \left[1 + 2\exp(-\frac{2\pi\zeta}{b}) \cos 2\pi\alpha \right], \tag{2.11}$$

and the Peierls energy and Peierls stress are given respectively by

$$E_{1p}^{(2)} = \frac{\mu b^2}{\pi(1-\nu)} \exp(-\frac{2\pi\zeta}{b}) \tag{2.12}$$

and

$$\sigma_{1p}^{(2)} = \frac{\mu}{1-\nu} \exp(-\frac{2\pi\zeta}{b}). \tag{2.13}$$

3 The generalized Peierls-Nabarro model using discrete Fourier transform

In this section, we present our generalized Peierls-Nabarro model for curved dislocations using the discrete Fourier transform, which incorporates the Peierls energies and Peierls stresses for both straight dislocations and dislocation kinks. The model is presented for dislocations in simple cubic crystals with the isotropy approximation, as in the classical Peierls-Nabarro model [1–3].

In a simple cubic crystal, let the coordinates axes coincide with the cubic axes, and the slip plane of the dislocation is located at $z = 0$. As in the classical Peierls-Nabarro model [1–3], the upper and lower halves of the crystal are assumed to be elastic continua governed by linear elasticity theory, and are connected at the slip plane by a nonlinear potential force. The total energy Eq. (2.1) is expressed in terms of the disregistry vector (ϕ, ψ) at the discrete lattice sites on the slip plane: (x_j, y_m) where $x_j = ja_1$ and $y_m = ma_2$ for integers j and m, where a_1 and a_2 are values of lattice spacing in the x and y axes, respectively. A constant shear stress $(\sigma_{13}^{\text{app}}, \sigma_{23}^{\text{app}})$ is applied to the system, and the uniform

shear state without dislocation under this applied stress is used as the reference state for the elastic energy E_{elastic} and the misfit energy E_{misfit}.

The elastic energy E_{elastic} given by Eq. (2.2) can be written as an integral over the slip plane. Replacing the integral by the summation at discrete lattice sites, we have

$$E_{\text{elastic}}=\sum_{j,m}\frac{a_1a_2}{2}[\sigma_{13}(x_j,y_m)\phi(x_j,y_m)+\sigma_{23}(x_j,y_m)\psi(x_j,y_m)]. \tag{3.1}$$

The stress components $\sigma_{13}(x_j,y_m)$ and $\sigma_{23}(x_j,y_m)$ can be obtained using the discrete Fourier transform under periodic boundary conditions. Under isotropic approximation, these two stress components can be given analytically in Fourier space by [32,33]

$$\widehat{\sigma}_{13}(k_1,k_2)=\mu\left(\frac{1}{2}\frac{k_2^2}{\|k\|}+\frac{1}{2(1-\nu)}\frac{k_1^2}{\|k\|}\right)\widehat{\phi}(k_1,k_2)+\frac{\nu\mu}{2(1-\nu)}\frac{k_1k_2}{\|k\|}\widehat{\psi}(k_1,k_2) \tag{3.2}$$

and

$$\widehat{\sigma}_{23}(k_1,k_2)=\frac{\nu\mu}{2(1-\nu)}\frac{k_1k_2}{\|k\|}\widehat{\phi}(k_1,k_2)+\mu\left(\frac{1}{2}\frac{k_1^2}{\|k\|}+\frac{1}{2(1-\nu)}\frac{k_2^2}{\|k\|}\right)\widehat{\psi}(k_1,k_2), \tag{3.3}$$

where $k=(k_1,k_2)$ are the frequencies in Fourier space, $\|k\|=\sqrt{k_1^2+k_2^2}$, $-\frac{N_1}{2}\le\frac{N_1a_1}{2\pi}k_1\le\frac{N_1}{2}-1$ and $-\frac{N_2}{2}\le\frac{N_2a_2}{2\pi}k_2\le\frac{N_2}{2}-1$, for a simulation cell with size $N_1a_1\times N_2a_2$ (N_1 and N_2 are even for numerical convenience), and a variable with hat represents its discrete Fourier transform. The constants in these two components of the self-stress of the dislocation are zero. Recall that the discrete Fourier transform is defined by, using ϕ as an example,

$$\widehat{\phi}(k_1,k_2)=\frac{1}{N_1N_2}\sum_{j=0}^{N_1-1}\sum_{m=0}^{N_2-1}\phi(x_j,y_m)e^{-i(k_1x_j+k_2y_m)}, \tag{3.4}$$

and the inverse discrete Fourier transform is given by

$$\begin{aligned}\phi(x_j,y_m)=&\sum_{\frac{N_1a_1}{2\pi}k_1=-N_1/2}^{N_1/2-1}\sum_{\frac{N_2a_2}{2\pi}k_2=-N_2/2}^{N_2/2-1}\widehat{\phi}(k_1,k_2)e^{i(k_1x_j+k_2y_m)},\\ &j=0,1,\cdots,N_1-1,\quad m=0,1,\cdots,N_2-1,\end{aligned} \tag{3.5}$$

both can be performed efficiently using the fast Fourier transform method (FFT). Note that $\widehat{\sigma}_{13}(k_1,k_2)=\widehat{\sigma}_{23}(k_1,k_2)=0$ when $\frac{N_1a_1}{2\pi}k_1=-\frac{N_1}{2}$ or $\frac{N_2a_2}{2\pi}k_2=-\frac{N_2}{2}$, for the correct symmetry of the highest frequencies [34].

In fact, in the above formulation, the elastic energy is obtained by connecting the disregistry vector $(\phi(x_j,y_m),\psi(x_j,y_m))$ smoothly using basis functions $e^{i(k_1x+k_2y)}$, $-\frac{N_1}{2}\le\frac{N_1a_1}{2\pi}k_1\le\frac{N_1}{2}-1$, $-\frac{N_2}{2}\le\frac{N_2a_2}{2\pi}k_2\le\frac{N_2}{2}-1$. The smooth disregistry, using component $\phi(x,y)$ as an example, is given by

$$\phi(x,y)=\sum_{\frac{N_1a_1}{2\pi}k_1=-N_1/2}^{N_1/2-1}\sum_{\frac{N_2a_2}{2\pi}k_2=-N_2/2}^{N_2/2-1}\widehat{\phi}(k_1,k_2)e^{i(k_1x+k_2y)}=\sum_{j=0}^{N_1-1}\sum_{m=0}^{N_2-1}\phi(x_j,y_m)f_{j,m}(x,y) \tag{3.6}$$

for $(x,y)\in[0,N_1a_1]\times[0,N_2a_2]$, where the basis functions $f_{j,m}(x,y)$, $0\le j\le N_1-1$, $0\le m\le N_2-1$, are given by

$$f_{j,m}(x,y)=\begin{cases}\dfrac{\sin\frac{\pi(x_j-x)}{a_1}\sin\frac{\pi(y_m-y)}{a_2}\cos\left[\frac{\pi(x_j-x)}{N_1a_1}+\frac{\pi(y_m-y)}{N_2a_2}\right]}{N_1N_2\sin\frac{\pi(x_j-x)}{N_1a_1}\sin\frac{\pi(y_m-y)}{N_2a_2}} & \text{if } x_j\neq x \text{ and } y_m\neq y,\\ \sin\dfrac{\pi(y_m-y)}{a_2}\left(N_2\tan\dfrac{\pi(y_m-y)}{N_2a_2}\right)^{-1} & \text{if } x_j=x \text{ and } y_m\neq y,\\ \sin\dfrac{\pi(x_j-x)}{a_1}\left(N_1\tan\dfrac{\pi(x_j-x)}{N_1a_1}\right)^{-1} & \text{if } x_j\neq x \text{ and } y_m=y,\\ 1 & \text{if } x_j=x \text{ and } y_m=y.\end{cases}\tag{3.7}$$

Note that in the summations with respect to k_1 and k_2 in Eq. (3.6), e^{ik_1x} is replaced by

$$\frac{1}{2}(e^{ik_1x}+e^{-ik_1x})\quad\text{when}\quad\frac{N_1a_1}{2\pi}k_1=-\frac{N_1}{2},$$

and e^{ik_2y} is replaced by

$$\frac{1}{2}(e^{ik_2y}+e^{-ik_2y})\quad\text{when}\quad\frac{N_2a_2}{2\pi}k_2=-\frac{N_2}{2},$$

for the correct symmetry of the highest frequencies [34]. The formulation of Eqs. (3.6) and (3.7) is used only when determining the exact location of the dislocation or in the analysis of the solutions, and is not for the purpose of numerical calculations. The numerical formulation has already been given in the previous paragraph.

The misfit energy Eq. (2.3) in the form of summation at the discrete lattice sites is

$$E_{\text{misfit}}=\sum_{j,m}a_1a_2[\gamma(\phi(x_j,y_m),\psi(x_j,y_m))-\gamma(\phi_0,\psi_0)],\tag{3.8}$$

where $\gamma(\phi,\psi)$ is the generalized stacking fault energy [17], and (ϕ_0,ψ_0) is disregistry vector in the uniform shear state under applied stress $(\sigma_{13}^{\text{app}},\sigma_{23}^{\text{app}})$:

$$\sigma_{13}^{\text{app}}+\frac{\partial\gamma}{\partial\phi}(\phi_0,\psi_0)=0,\quad\sigma_{23}^{\text{app}}+\frac{\partial\gamma}{\partial\psi}(\phi_0,\psi_0)=0.$$

Under applied stress $(\sigma_{13}^{\text{app}},\sigma_{23}^{\text{app}})$, the equilibrium configuration of the dislocation is determined by minimizing the potential energy functional

$$E=E_{\text{elastic}}+E_{\text{misfit}}+\sum_{j,m}a_1a_2[\sigma_{13}^{\text{app}}\phi(x_j,y_m)+\sigma_{23}^{\text{app}}\psi(x_j,y_m)]\tag{3.9}$$

with respect to $\phi(x_j,y_m)$ and $\psi(x_j,y_m)$, where E_{elastic} and E_{misfit} are given by Eqs. (3.1) and (3.8), respectively. The resulting equations are

$$\begin{cases} \sigma_{13}(x_j,y_m)+\dfrac{\partial\gamma}{\partial\phi}(\phi(x_j,y_m),\psi(x_j,y_m))+\sigma_{13}^{\text{app}}=0, \\ \sigma_{23}(x_j,y_m)+\dfrac{\partial\gamma}{\partial\psi}(\phi(x_j,y_m),\psi(x_j,y_m))+\sigma_{23}^{\text{app}}=0. \end{cases} \tag{3.10}$$

The solutions $\phi(x_j,y_m)$ and $\psi(x_j,y_m)$ are found by solving the following dynamic equations which minimize the total energy in the steepest descent direction to the equilibrium state

$$\begin{cases} \dfrac{\partial\phi(x_j,y_m,t)}{\partial t}=-\sigma_{13}(x_j,y_m,t)-\dfrac{\partial\gamma}{\partial\phi}(\phi(x_j,y_m,t),\psi(x_j,y_m,t))-\sigma_{13}^{\text{app}}, \\ \dfrac{\partial\psi(x_j,y_m,t)}{\partial t}=-\sigma_{23}(x_j,y_m,t)-\dfrac{\partial\gamma}{\partial\psi}(\phi(x_j,y_m,t),\psi(x_j,y_m,t))-\sigma_{23}^{\text{app}}. \end{cases} \tag{3.11}$$

4 Peierls stress and Peierls energy for straight dislocations

In this section, we apply our model to the straight edge and screw dislocations and compare the results with the classical Peierls-Nabarro model.

Assume that the straight dislocation lies parallel to the y axis. Only the disregistry in the direction of the Burgers vector is considered, and the Frenkel sinusoidal potential Eq. (2.4) is used for the nonlinear interplanar interaction, where the interplanar distance $d=b$. For a straight edge dislocation, the Burgers vector is in the direction of the x axis,

$$\phi=\phi(x),\quad \tau=\sigma_{13}^{\text{app}},\quad \psi=0,\quad \sigma_{23}^{\text{app}}=0.$$

For a straight screw dislocation, the Burgers vector is in the direction of the y axis,

$$\psi=\psi(x),\quad \tau=\sigma_{23}^{\text{app}},\quad \phi=0,\quad \sigma_{13}^{\text{app}}=0,$$

and the Frenkel potential Eq. (2.4) is a function of ψ. The system in Eq. (3.11) is then reduced to a single equation in one dimension for the disregistry $\phi(x)$ (edge) or $\psi(x)$ (screw). We consider the cases of $b=2a_1$ and $b=a_1$ corresponding to the periods $b/2$ (Eq. (2.8)) and b (Eq. (2.11)) in misfit energy in the classical Peierls-Nabarro model, respectively, and use simulation cells with 1024 atoms and 512 atoms for these two cases, respectively. The difference of the disregistry at the two end points of the simulation cell is b, and in order to meet the periodic boundary conditions, a linear function is subtracted before the discrete Fourier transform is performed. Further increasing the size of simulation cells only gives negligible changes in the results. We choose $\nu=0.347$ which is the value for Al.

Following [20,23,24], the Peierls stress, denoted by σ_{1p}, is defined as the critical value of the applied stress above which the equilibrium profile of the dislocation no longer

Table 1: Peierls stress.

	$\sigma_{1p}(b=2a_1)$	$\sigma_{1p}^{(1)}$	$\sigma_{1p}(b=a_1)$	$\sigma_{1p}^{(2)}$
Edge	$7.4\times10^{-5}\mu$	$2.1\times10^{-4}\mu$	0.0051μ	0.0127μ
Screw	$1.4\times10^{-3}\mu$	$3.7\times10^{-3}\mu$	0.0192μ	0.0429μ

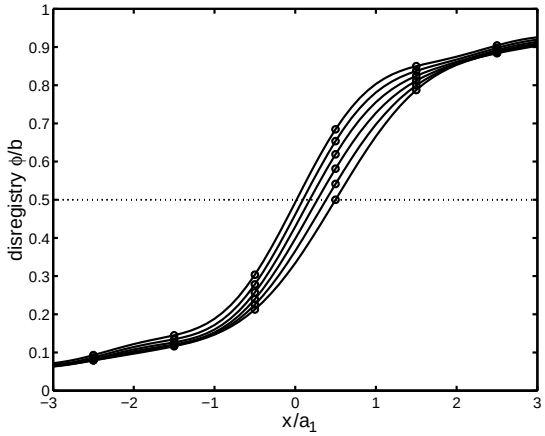

Figure 1: The disregistry profiles when an edge dislocation ($b=a_1$) is located at different positions. The circles denote the disregistry values on atom positions.

exists. Our calculated values of the Peierls stress for the cases $b=2a_1$ and $b=a_1$ are shown in Table 1. It can be seen that these results agree in order of magnitude with the corresponding values of $\sigma_{1p}^{(1)}$ and $\sigma_{1p}^{(2)}$ in the classical Peierls-Nabarro models given by Eq. (2.10) and Eq. (2.13), respectively. Note that for the screw dislocation, the coefficient $\mu/(1-\nu)$ in Eqs. (2.10) and (2.13) should be replaced by μ.

We have also studied the disregistry profiles and the variation in the total energy when the dislocation is located at different positions relative to the lattice sites, for which different values of applied stress are required. The center of the dislocation is determined by

$$\bar{x}=N_1a_1-\sum_{j=0}^{N_1}\phi(x_j)a_1/b,$$

which is equivalent to the definition given in [20]:

$$\bar{x}=\sum_{j=0}^{N_1}x_j\rho(x_j)a_1/b,$$

where $\rho(x)=\phi'(x)$ is the dislocation density. In order to obtain the disregistry profiles when the dislocation center is located at different positions, we fix the disregistry of an atom nearest to the dislocation center (the atom at $1/2$ in the rescaled unit in Fig. 1) by adding a constant in disregistry at each time step, and the value of the applied stress

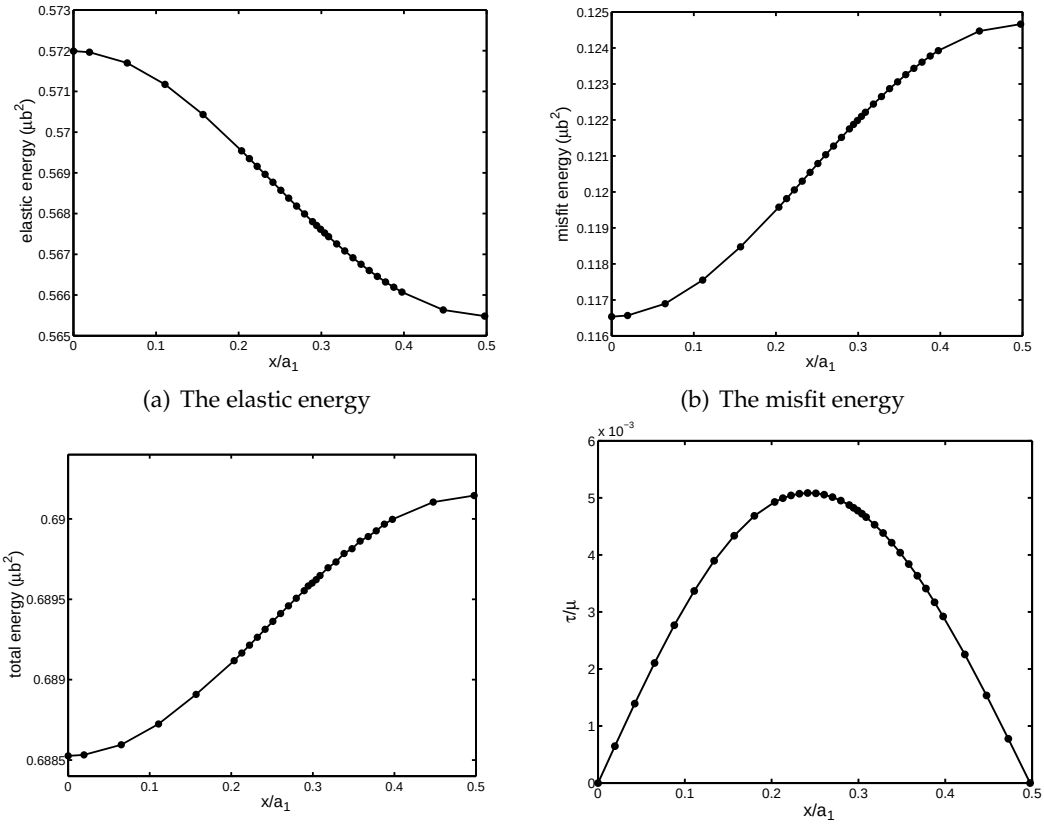

(a) The elastic energy (b) The misfit energy

(c) The total energy (d) The applied stress

Figure 2: The variations in the energies and the required applied stress when the center of the edge dislocation ($b = a_1$) is located at different positions.

is obtained accordingly. Continuous disregistry profiles are obtained from the values at discrete lattice sites using Eqs. (3.6) and (3.7).

The results for the disregistry profiles and the variation in the total energy of an edge dislocation when $b = a_1$ are shown in Figs. 1 and 2. Without applied stress, a stable solution is found, whose center stays in the middle between two atoms, and whose total energy is minimal, see the leftmost profile in Fig. 1 and the total energy in Fig. 2(c). When the center of the dislocation moves to the position of an atom, the total energy is maximal, see the rightmost profile in Fig. 1 and the total energy in Fig. 2(c). These results agree with those from the classical Peierls-Nabarro model Eq. (2.11). Unlike the assumption in the classical Peierls-Nabarro model, the disregistry profiles are not exact rigid shifts from the profile without applied stress, see Fig. 1. As the center of the dislocation moves from the middle of two adjacent atoms to the position of an atom, the total energy (Fig. 2(c)) and the misfit energy (Fig. 2(b)) increase, while the elastic energy (Fig. 2(a)) decreases. The values of applied stress required to obtain these disregistry profiles are shown in

Table 2: Peierls energy (in unit of μb^2) for the case $b=2a_1$.

	$\Delta E_{\text{elastic}}$	ΔE_{misfit}	E_{1p} (ΔE_{total})	PN ($E_{1p}^{(1)}$)
Edge	-1.0×10^{-4}	1.1×10^{-4}	1.2×10^{-5}	3.3×10^{-5}
Screw	-1.3×10^{-3}	1.5×10^{-3}	2.3×10^{-4}	6.0×10^{-4}
Edge (rigid shift)	-2.1×10^{-5}	3.3×10^{-5}	1.2×10^{-5}	
Screw (rigid shift)	-3.7×10^{-4}	6.0×10^{-4}	2.3×10^{-4}	

Table 3: Peierls energy (in unit of μb^2) for the case $b=a_1$.

	$\Delta E_{\text{elastic}}$	ΔE_{misfit}	E_{1p} (ΔE_{total})	PN ($E_{1p}^{(2)}$)
Edge	-0.0065	0.0081	0.0016	0.0040
Screw	-0.0147	0.0209	0.0061	0.0138
Edge (rigid shift)	-0.0024	0.0040	0.0016	
Screw (rigid shift)	-0.0077	0.0138	0.0061	

Fig. 2(d). Note that in Figs. 1 and 2, the origin of the x axis is moved to the center of the dislocation without applied stress.

The Peierls energy is determined by the difference between the maximum and minimum of the total energy. The evaluated values of the Peierls energy E_{1p} (ΔE_{total}) and the change of the elastic energy ($\Delta E_{\text{elastic}}$) and misfit energy ($\Delta E_{\text{misfit}}$) for different cases are presented in Tables 2 and 3. It can be seen that $\Delta E_{\text{elastic}}$ and ΔE_{misfit} have the same order of magnitude and opposite signs, which results in a smaller ΔE_{total} due to their cancellation. The obtained values of the Peierls energy E_{1p} for different cases agree in order of magnitude with the analytical predictions in the classical Peierls-Nabarro models (PN) given by Eq. (2.9) or Eq. (2.12), in which only the variation in the misfit energy is considered when the dislocation is shifted rigidly. The cancellation in $\Delta E_{\text{elastic}}$ and ΔE_{misfit} is consistent with the results obtained by Schoeck in [25] using approximations of Poisson's summation formula and the arctangent type trial functions.

To further compare our model with classical Peierls-Nabarro model, we also calculate the variations of the energies when the dislocation undergoes rigid shift. The results are also shown in Tables 2 and 3. It is interesting to find that the Peierls energy obtained using our full model agrees excellently with that from simple shifting. Another interesting fact is that ΔE_{misfit} obtained using our model with approximation of simple shift agrees excellently with the Peierls energy from the classical Peierls-Nabarro model. This shows that our model is indeed a generalization of the classical Peierls-Nabarro model.

In summary of this section, we have validated our model by showing that our model, which incorporates more physics such as the variations in the dislocation profile and the elastic energy, is a direct generalization of the classical Peierls-Nabarro model, which has been shown to give qualitative descriptions of the dislocation structure and mobility [14–16]. Even though the results of the Peierls energy and Peierls stress for straight

dislocations obtained using our model are not significantly different from those from the classical Peierls-Nabarro model, our model is able to calculate the Peierls energy and Peierls stress for dislocation kinks in the same manner as those for straight dislocations, which has never been done in the literature.

5 The second Peierls stress and the second Peierls energy for dislocation kinks

In this section, we present the simulation results using our model on the second Peierls stress and the second Peierls energy for dislocation kinks. We consider an edge dislocation with a double kink. Assume that the almost straight edge dislocation lies parallel to the y axis, and the Burgers vector is in the direction of the x axis. We use the isotropic elasticity and consider only the disregistry in the direction of Burgers vector (i.e., $\psi=0$). The Frenkel sinusoidal potential Eq. (2.4) is still employed for the interplanar atomic interaction. The dynamics equation under these simplified conditions is

$$\frac{\partial}{\partial t}\phi(x_j,y_m,t)=-\sigma_{13}(x_j,y_m,t)-\frac{\mu b}{2\pi d}\sin\frac{2\pi\phi(x_j,y_m)}{b}-\sigma_{13}^{\text{app}}, \tag{5.1}$$

where $\sigma_{13}(x_j,y_m,t)$ is given by Eq. (3.2) with $\psi=0$. The lattice constants in the slip plane are $a_1=a_2=b$, and the simulation cell is $512b\times512b$. The Poisson ratio $\nu=0.347$. The straight parts of the dislocation lie in adjacent Peierls valleys. Since we are interested in the properties of a single kink, the two kinks in the dislocation are placed at a distance of one half of the size of the simulation cell to reduce the interaction effect between them. Further increase in the size of simulation cell (thus the distance between the two kinks) only gives negligible changes in the results. As in the cases of straight dislocations, the difference of the disregistry at the two boundaries of the simulation cell in the direction of the x axis is b, and in order to meet the periodic boundary conditions, a linear function is subtracted before the discrete Fourier transform is performed.

We first investigate the equilibrium configuration of the kink without applied stress. Fig. 3 shows the profiles of the disregistry of the kinked dislocation for different values of interplanar distance, in which the continuous disregistry profiles are obtained from the values at discrete lattice sites using Eqs. (3.6) and (3.7). Fig. 3 also shows the location of the dislocation line, which is identified by the contour line $\phi=b/2$. The center of the kink is identified by the intersection point of the kink with the atomic row between the two Peierls valleys where the straight parts of the dislocation are located, see Fig. 4. Without applied stress, the center of the kink stays in the middle of two adjacent atomic sites, see also Fig. 4. From Fig. 3 we can see that when the interplanar distance d is smaller, the kink is narrower, which agrees with the conclusion from the classical Peierls-Nabarro model (Eq. (2.9) or (2.12)) that smaller d gives higher Peierls energy thus longer part of the dislocation stays in the Peierls valley. Following [1,6,8,9,13], we determine the width of the kink by $w=b/\tan\theta_m$, where $\tan\theta_m$ is the maximum slope of the kink, see Fig. 4. The

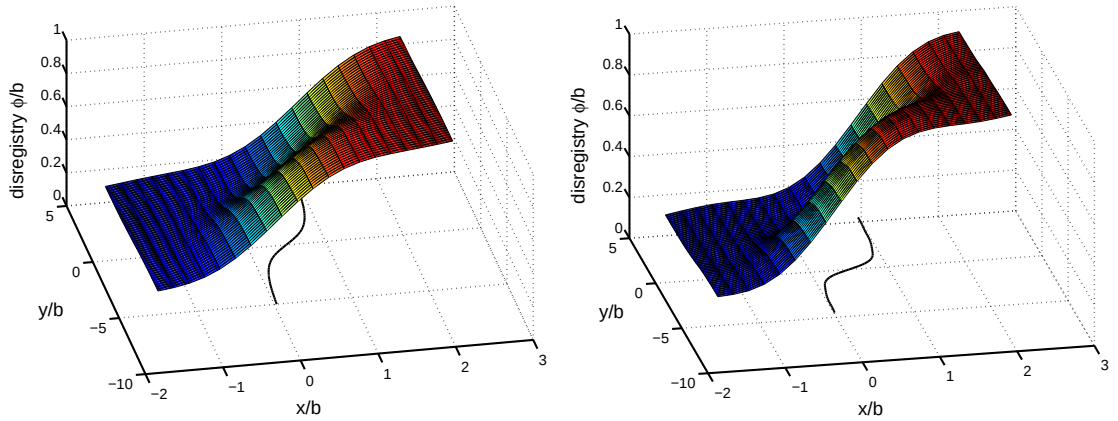

(a) $d=b$ (b) $d=\sqrt{\frac{2}{3}}b$

Figure 3: The disregistry configurations for a kink in an edge dislocation and locations of the dislocation line.

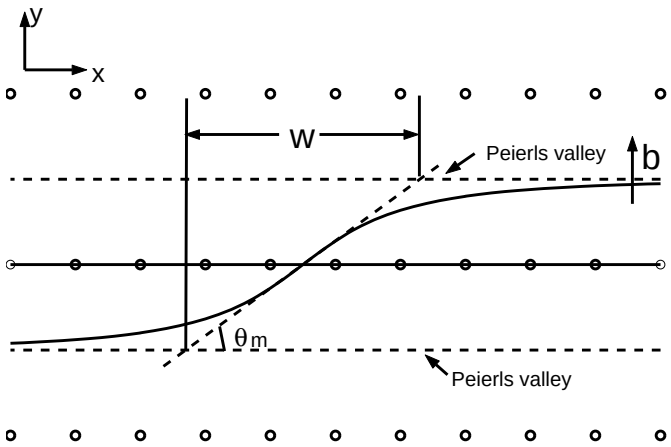

Figure 4: The definition of the kink width and the center of the kink. The kink width $w=b/\tan\theta_m$. The circles show the positions of the atoms in a cubic crystal. The horizontal dash lines indicate the locations of the Peierls valleys. The center of the kink is identified by the intersection point of the kink with the atomic row between the two Peierls valleys where the straight parts of the dislocation are located.

evaluated kink width is about $3.5b$ in Fig. 3(a) for the case of $d=b$, and $2.0b$ in Fig. 3(b) for the case of $d=\sqrt{2/3}b$. Note that in Fig. 3 and all other figures in this section, the x axis is shifted to a Peierls valley where part of the dislocation lies, and the y axis is shifted to the center of the kink without applied stress.

Similar to the Peierls stress for a straight dislocation, the second Peierls stress for a dislocation kink is defined as the critical value of the applied stress above which no stable equilibrium configuration of the kinked dislocation exists. Physically, above this critical value of the applied stress, the kink can move over the energy barrier. In the case

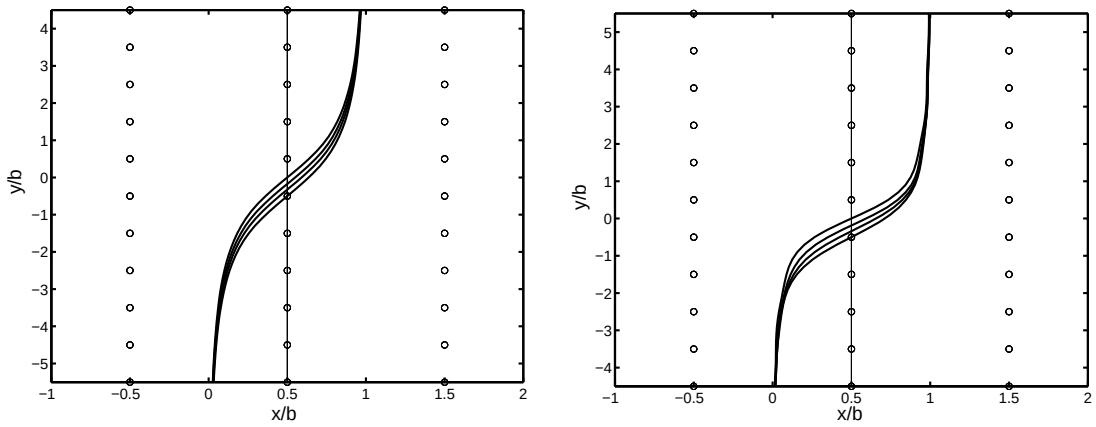

(a) d=b (b) d=$\sqrt{\frac{2}{3}}$b

Figure 5: The dislocation profiles when the kink is located at different positions.

of $d=b$, the obtained second Peierls stress is $\sigma_{2p}=3.2\times10^{-6}\mu$, which is several orders of magnitude smaller than the corresponding Peierls stress for straight dislocations shown in Table 1 (our result σ_{1p} for the case $b=a_1$ and the result of classical Peierls-Nabarro model $\sigma_{1p}^{(2)}$). In the case of a smaller interplanar distance $d=\sqrt{2/3}b$ (thus a narrower kink), the evaluated second Peierls stress is $\sigma_{2p}=3.7\times10^{-4}\mu$, which is much larger than that in the case of $d=b$. In the case of $d=\sqrt{2/3}b$, from the classical Peierls-Nabarro model, $\sigma_{1p}^{(2)}=0.63\mu$ for a straight edge dislocation, and the second Peierls stress for a kink is also several orders of magnitude smaller than the Peierls stress for straight dislocations.

We have also studied the dislocation profiles and the variation in the total energy when the kink is located at different positions relative to the lattice sites, for which different values of applied stress are required. In order to obtain the disregistry profiles when the kink center is located at different positions, we fix the disregistry of an atom nearest to the kink center by adding a constant in disregistry at each time step, and the value of the applied stress is obtained accordingly. Since there are two kinks in the dislocation line and they are symmetric with respect to the central line of the simulation cell parallel to the x axis, we only evolve the disregistry of half of the atoms in the simulation cell and the values on the other half are determined by reflection.

Fig. 5 shows the dislocation profiles when the kink is located at different positions for the cases of $d=b$ and $d=\sqrt{2/3}b$. The uppermost profiles in Fig. 5(a) and (b) are the stable profiles without applied stress. The second Peierls energy for the dislocation kink is determined by the difference between the maximum and minimum of the total energy as the kink moves along the dislocation. The obtained second Peierls energy in our simulations is $E_{2p}=7.5\times10^{-7}\mu b^3$ for the case of $d=b$ and $E_{2p}=1.2\times10^{-4}\mu b^3$ for the case of $d=\sqrt{2/3}b$. The variations in the elastic energy, misfit energy and total energy, and the applied stress required when the kink is located at different positions are shown

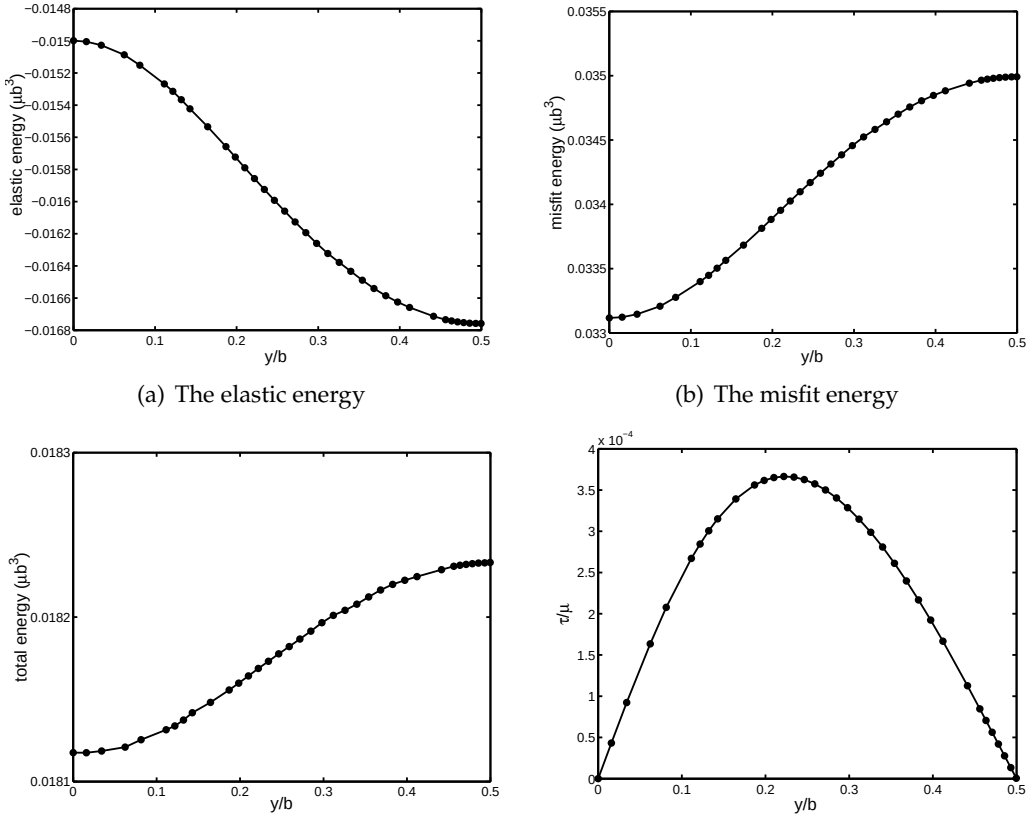

(a) The elastic energy (b) The misfit energy

(c) The total energy (d) The applied stress

Figure 6: The variations in the elastic energy, misfit energy and total energy, and the applied stress required when the kink center in an edge dislocation is located at different positions for the case of $d=\sqrt{\frac{2}{3}}b$.

in Fig. 6 for the case of $d=\sqrt{2/3}b$. Similar to the energies of a straight dislocation, as the dislocation kink moves from the middle of two adjacent atoms to the position of an atom, the total energy (Fig. 6(c)) and the misfit energy (Fig. 6(b)) increase, while the elastic energy (Fig. 6(a)) decreases.

We have also calculated the second Peierls energy using rigid shift of the kink profile without applied stress. The results are $1.2\times10^{-6}\mu b^3$ and $2.2\times10^{-4}\mu b^3$ for the cases of $d=b$ and $d=\sqrt{2/3}b$, respectively. These results are of the same order of magnitude as those obtained using the full relaxation shown above.

Now we compare our model with a recent Frenkel-Kontorowa model for kinked dislocation using string approximation and line tension model [9]. The limitations of these type of models have been discussed in the introduction. In [9], the dislocation profile is obtained by the balance between the line tension and the potential force due to the periodic variation of the total energy when the straight dislocation moves over the discrete

lattice, and the second Peierls stress and second Peierls energy for a dislocation kink are obtained by leading order approximation using rigid shift of the kink profile without applied stress. Their obtained kink profile, using the notations in this paper and $a_1=a_2=b$, is

$$f(y)=\frac{2b}{\pi}\tan^{-1}e^{\pi y/w},$$

where $w=\sqrt{\Gamma/(2E_{1p})}b$ is the width of the kink, Γ is the line energy, and E_{1p} is the Peierls energy. Their obtained second Peierls energy and second Peierls stress for a dislocation kink are

$$E_{2p}=16e^{-\pi w/b}\Gamma b,\quad \sigma_{2p}=16\pi e^{-\pi w/b}\Gamma/b^2,$$

respectively. The two models agree in some qualitative properties of dislocation kinks such as higher Peierls energy gives narrower kink.

One limitation of the line tension model is that the line energy cannot be determined accurately for a general curved dislocation due to the long-range elastic interaction [1]. Our model can be used to examine the line tension approximation and to determine the value of the line energy in the Frenkel-Kontorowa model for kinked dislocation. Using the same value of the kink width w, the fitted value of the line energy using our model is about $0.1\mu b^2$ for the edge dislocation and $0.2\mu b^2$ for the screw dislocation. With this fitted line energy, for the kink with width $w=3.5b$ in the edge dislocation when $d=b$, the second Peierls energy and second Peierls stress given by the formulas in [9] are $E_{2p}=2.4\times10^{-5}\mu b^3$ and $\sigma_{2p}=7.5\times10^{-5}\mu$, which are larger by at least one order of magnitude than our results. Qualitatively, their second Peierls stress is also several orders of magnitude smaller than the Peierls stress for straight dislocations (see Table 1), which agrees with the results of our model.

For the realistic FCC or covalent bond materials, the generalization of our model to triangular lattice in the slip plane is needed. This work is in progress and the results will be reported elsewhere. Now, as an example, using the present model, we may roughly estimate the second Peierls energy and the second Peierls stress for a kink in 90^o glide partial dislocation in Si. We use the isotropic elastic constants $\mu=0.425\text{eV}/\text{Å}^3$ and $\nu=0.218$ [1]. The length of the Burgers vector of the perfect dislocation is $b=3.84$Å and that of a partial dislocation is $b_p=b/\sqrt{3}$. The lattice spacing perpendicular to the slip plane is $d=\sqrt{1/24}b$, and lattice constants $a_1=\sqrt{3}b/2$ and $a_2=b$. Our evaluated second Peierls energy for a kink in this partial using rigid shift approximation is 1.5eV, which agrees with the values of 0.5-0.6eV obtained using atomistic simulations [35] and is in the range of 1.0-1.7eV for the second Peierls energy for dislocation kink (the kink migration energy) in Si obtained from experiments [36,37]. Our evaluated second Peierls stress for this kink is 0.2μ, which has the same order of magnitude as the result $0.358J$ ($J=0.536\text{eV}/\text{Å}^3$ is the anisotropic elastic dislocation energy factor) obtained using the Frenkel-Kontorowa model in [9].

6 Summary and discussions

We have proposed a generalized Peierls-Nabarro model for curved dislocations incorporating the Peierls energies and Peierls stresses. In our model, the elastic energy is calculated efficiently using the discrete Fourier transform, the core structure of curved dislocations is incorporated, and the discreteness in both elastic energy and misfit energy is considered. Our model is validated by comparisons with the classical Peierls-Nabarro model for straight dislocations. Simulation results show that our model gives some interesting predictions for the energy barriers and critical stresses for the motion of kinked dislocations, which agree qualitatively with the results from experiments and atomistic simulations. We have also examined using our model the Frenkel-Kontorowa model for kinked dislocations using string approximation and line tension model [9].

The generalization of our model will be done in the future work to include the elastic anisotropy, the generalized stacking fault energy [17] obtained accurately using *ab initio* calculations [18–23] for the interplanar atomic interaction, and the realistic lattices in the slip plane such as triangular lattice in FCC or covalent bond crystals.

Acknowledgments

The work of Y. Xiang is partially supported by the Hong Kong Research Grants Council CERG 603706. The work of P.B. Ming is partially supported by the National Natural Science Foundation of China under the grant 10571172 and is also supported by the National Basic Research Program under the grant 2005CB321704.

References

[1] J. P. Hirth and J. Lothe, *Theory of Dislocations*, 2nd ed., (John Wiley, New York, 1982).
[2] R. E. Peierls, *Proc. Phys. Soc.*, **52**(1940), 23.
[3] F. R. N. Nabarro, *Proc. Phys. Soc.*, **59**(1947), 256.
[4] H.B. Huntington, *Proc. Phys. Soc. B*, **68**(1955), 1043.
[5] J. E. Dorn and S. Rajnak, *Trans. AIME*, **230**(1964), 1052.
[6] G. Schottky, *Phys. Stat. Solidi*, **5**(1964), 697.
[7] W. T. Sanders, *J. Appl. Phys.*, **36**(1965), 2822.
[8] A. Seeger and P. Schiller, in *Physical Acoustics*, IIIA, ed. W.P. Mason, (Academic Press, New York, 1966).
[9] B. Joos and M. S. Duesbery, *Phys. Rev. B*, **55**(1997), 11161.
[10] B. Joos and J. Zhou, *Phil. Mag. A*, **81**(2001), 1329.
[11] A. Seeger, *Mater. Sci. Eng. A*, **370**(2004), 50.
[12] W. Cai, V.V. Bulatov, J. Chang, J. Li, and S. Yip, in *Dislocations in Solids*, Vol. 12, ed. F.R.N. Nabarro and J. P. Hirth, (North-Holland, Amsterdam, 2004).
[13] W. T. Read, Jr., *Dislocations in Crystals*, (McGraw-Hill, New York, 1953).
[14] F. R. N. Nabarro, *Mater. Sci. Eng. A*, **234-236**(1997) 67.
[15] F. R. N. Nabarro, *Phil. Mag. A*, **75**(1997), 703.

[16] B. Joos and M. S. Duesbery, *Phys. Rev. Lett.*,**78**(1997), 266.
[17] V. Vitek, *Phil. Mag.*, **18**(1968), 773.
[18] E. Kaxiras and M. S. Duesbery, *Phys. Rev. Lett.*, **70**(1993), 3752.
[19] B. Joos, Q. Ren, and M. S. Duesbery, *Phys. Rev. B*, **50**(1994), 5890.
[20] V. V. Bulatov and E. Kaxiras, *Phys. Rev. Lett.*, **78**(1997), 4221.
[21] J. Hartford, B. von Sydow, G. Wahnstrom, and B.I. Lundqvist, *Phys. Rev. B*, **58**(1998), 2487.
[22] O. N. Mryasov, Y. N. Gornostyrev, and A. J. Freeman, *Phys. Rev. B*, **58**(1998), 11927.
[23] G. Lu, N. Kioussis, V. V. Bulatov, and E. Kaxiras, *Phys. Rev. B*, **62**(2000), 3099.
[24] A. B. Movchan, R. Bullough, and J. R. Willis, *Eur. J. Appl. Math.*, **9**(1998), 373.
[25] G. Schoeck, *Phil. Mag. A*, **79**(1999), 2629.
[26] G. Schoeck, *Phil. Mag. A*, **82**(2002), 1033.
[27] G. Schoeck and M. Krystian, *Phil. Mag.*, **85**(2005), 949.
[28] V. V. Bulatov, S. Yip, and A. S. Argon, *Phil. Mag. A*, **72**(1995), 453.
[29] A. B. Movchan, R. Bullough, and J. R. Willis, *Phil. Mag.*, **83**(2003), 569.
[30] Y. Xiang, *Commun. Comput. Phys.*, **1** (2006), 383.
[31] G. Xu and A. S. Argon, *Phil. Mag. Lett.*, **80**(2000), 605.
[32] Y. Xiang, H. Wei, P. B. Ming, and W. E, *Acta Mater.*, to appear, 2008.
[33] T. Mura, *Micromechanics of Defects in Solids*, (Martinus Nijhoff Publishers, Dordrecht, 1987).
[34] L. N. Trefethen, *Spectral Methods in MATLAB*, (SIAM, Philadelphia, 2000).
[35] J. F. Justo, V. V. Bulatov, and S. Yip, *J. Appl. Phys.*, **86**(1999), 4249.
[36] H. Alexander and H. Teichler, in *Materials Science and Technology*, Vol.4, edited by R. W. Cahn, P. Haasen, and E. J. Kramer (VCH Weinheim, 1991).
[37] B. Y. Farber, Y. L. Iunin, and V. I. Nikitenko, *Phys. Status Solidi A*, **97**(1986), 469.